Article:

Tang, N., Soltani, P., Pinna, C. orcid.org/0000-0002-9079-1381 et al. (2 more authors) (2018) Ageing of a polymeric engine mount investigated using digital image correlation. Polymer Testing, 71. pp. 137-144. ISSN 0142-9418

https://doi.org/10.1016/j.polymertesting.2018.08.036

Ageing of a polymeric engine mount investigated using digital image correlation

Ning Tang[a,*], Payam Soltani[b], Christophe Pinna[a], David Wagg[a], Roly Whear[c]

[a]*Department of Mechanical Engineering, The University of Sheffield, Sheffield, S1 3JD, UK.*
[b]*School of Mechanical, Aerospace and Automotive Engineering, Coventry University, Coventry, CV1 5FB, UK.*
[c]*Jaguar Land Rover Ltd, CV35 ORR, UK.*

Abstract

Polymeric engine mounts have been widely used as vibration isolators in vehicles. In general, understanding ageing-dependent stiffness is important for life cycle design. In this paper, a new experimental procedure is developed to study the ageing mechanisms of service-aged engine mounts using digital image correlation measurements. The present contribution demonstrates that the leading factors for ageing-dependent stiffness are, not only the elastic modulus variation, but also the creep deformation and micro-structural change. The results show that pure thermal effects, such as that used to simulate ageing, leads to a uniform change in the rubber component inside the mount. This is not the same as the service-aged mount behaviour. In addition, the cross-sectional creep deformation dominates the increase in rigidity. Finally, the results suggest that micro-structural change may also lead to the stiffness variation of the mounts with high working mileage.

Key words: elastomer ageing, engine mount, digital image correlation

1. Introduction

Elastomeric engine mounts have been used for many years as isolators for internal combustion engines. Their dynamic performance changes with operation time. Although this variation may not shift the resonance frequencies of the isolator that significantly, their change in performance does lead to more vibration energy being transferred into the vehicle. As a result, this variation is harmful to the overall vehicle and to the ride comfort, and therefore is of interest to the designer.

Several numerical and experimental prediction methods for engine mounts have been developed over the past decade [1-4]. Most of these studies pointed out that nonlinear stiffness should ideally be predictable, in order to design the dynamic characteristics. Understanding the factors that influence the elasticity of the engine mount becomes, therefore, essential, especially for a service-aged engine mount.

Thermal ageing is one of the main ageing mechanisms for an engine mount [5]. Thermal ageing is caused by the combination of oxidation, weakening of the reinforcing filler network and chemical degradation of the polymer network. Chemical degradation occurs through chain scissions and cross-linking, which alters the elastomer's stiffness. The rate at which these reactions occurs is dependent on the ambient conditions; temperature and humidity [6,7]. Generally, chain scission will soften the elastomers as the backbone covalent bonds rupture [8], while, cross-linking stiffens the aged elastomer due to the creation of bonds between two adjacent polymer chains [7]. During ageing both these chemical degradation mechanisms occur although one process typically dominates. This depends on the chemical compounds of the material, especially the additives of the rubber [9].

Cyclic loading is one of the other important factors when studying the ageing behaviour for engine mounts. The influences of harmonic excitation have been studied in [10,11]. Under dynamic loading, the breakage of a carbon black filler network is an additional significant factor for creating stiffness variation. However, no unique correlation between ageing time and stiffness has yet been found for different types of elastomers [5,12-15].

Most research focused on the ageing of the elastomer in an engine mount is carried out under laboratory conditions. The test specimens are normally prepared based on the ISO:23529 standard [16]. As a result, the sample size is much smaller than the rubber used in a real engine mount. The rate of heat flow inside the elastomer is, therefore, much higher for a laboratory sample. This difference in thermal conditions introduces significant uncertainties into the estimation of stiffness variations. Furthermore, the engine mount experiences cyclic loadings closer to random frequencies and magnitudes in practice. As a result,

* Corresponding author:
E-mail address: tang.n1988@gmail.com, n.tang@sheffield.ac.uk.

the imposed dynamic force profiles under laboratory conditions differ from those in a practical service-aged engine mount, which causes further difficulty in estimating the stiffness variation. Therefore, an investigation into the mechanics of stiffness variation for a real engine mount is needed.

This paper investigates the ageing mechanisms including, geometric and micro-structural variation, for a service-aged engine mount using digital image correlation (DIC) observations. A new experimental procedure has been developed to measure the cross-sectional deformation of the elastomer from both new and aged engine mounts with the characterisation of full-field strain distributions using DIC. This paper starts with a correlation of the physical ageing indicators such as mileage of a vehicle and unladen height of the main spring to the dynamic characteristic of interest, namely stiffness. The second part of this study focuses on how the creep deformation and micro-structural change influence the overall stiffness in a service-aged engine mount. Finally, a feasibility study was conducted on whether a laboratory accelerated thermal ageing test can simulate the micro-structural and geometric variations of a service-aged mount.

2. Material and methods

2.1. Investigated engine mounts

The engine mounts studied in this research were commercial products fitted to a particular Land Rover model. A representative sample is shown in Figure 1. For the purpose of the ageing studies undertaken, some samples were removed from vehicles which had been used in high temperature environments.

Figure 1: Hydraulic engine mount and its components.

The engine mount studied in this paper is made from four components: the main spring, the inertia track and decoupler, the viscous liquid chamber and a steel case. The main spring contributes to the elasticity of the entire mount. This spring is divided into three components: the tip, the rib and the elastomeric element. The main load-carrying region of an engine mount is located between the tip and the rib, as shown in Figure 1(b). Since the load-carrying region is axisymmetric, test results on half of the cross-section are assumed to represent the overall performance in the following analysis. The axisymmetric axis here is defined as the central axis of the engine mount.

In this study, four different mounts with different in-service ageing conditions were investigated. The basic properties of these mounts are listed in Table 1.

Table 1: Basic properties of engine mount samples

sample	aged time, days	service mileage, km	unladen gap, mm
1	0	0	11.5
2	51	0	11
3	unknown	129,996	5.4
4	unknown	70,600	3.1

The unladen gap refers to the maximum distance that each engine mount can be compressed. Sample 1 is a new engine mount used as a reference mount. Sample 2 is a mount thermally aged under laboratory conditions by exposure in a thermal chamber to a temperature of 100 ^{o}C for 51 days. This sample was used to separate the influences of thermal effects from practical service ageing. Samples 3 and 4 are two service-aged engine mounts that were disassembled from real vehicles. The operating temperature for the engines in these vehicles was in a range from 80 ^{o}C to 120 ^{o}C. In a real vehicle, service mileage rather than time-in-service is selected as an indicator for the effective working time. The reasons are as follows; time-in-service represents the overall vehicle life, regardless of whether the vehicle is in operation. During engine operation the thermal effects are at their highest. This accelerates the rate at which the elastomer ages significantly. Therefore, the real operational time of the vehicle is proportional to the travelled distance (or mileage) and is, therefore, a more realistic and important ageing indicator. As a result, service mileage can be treated as a physical parameter that is easy to measure and can represent real operation time.

2.2. Static compression tests

Static compression tests were carried out using a uni-axial test machine to obtain the engine mounts' load-deflection data in the axial direction. A Tinius-Olsen machine was used for this work which was comprised of a self-contained electric power unit, a load frame with a cross-head mounted actuator and a closed-loop controller. A 25 kN-capacity load cell was attached between the upper grip and the compressing plate. In operation, the position of the upper grip was measured using a linear voltage differential transformer.

Tests were carried out by applying a static compression range between 0 to 4 mm at a loading speed of 5 mm/min. A preload of 3 N was applied on the engine mount to ascertain the initial contact. The local tangent stiffness was obtained using the differential of the load-deflection relationship. The linear stiffness here is defined as the average of the local tangent stiffness values for the selected static compression range.

2.3. Static compression tests on main spring with digital image correlation

The main spring of the engine mount was cut into two parts in order to access the internal strain distributions in the cross-sections. Since the main spring is comprised of both polymeric and metal components, uniform flatness and avoidance of excessive deformation during the cutting process are of great importance. The detailed procedures for sample preparations were as follows;

- The viscous liquid in the full mount was first drained. A small hole with a diameter of 5 mm was drilled in the bottom of the mount, and the mount was allowed to drain for 24 hours.
- The outer case was cut using a hacksaw. Following this, the engine mount was disassembled, and the main spring was extracted. Dry, clean sand was then used to absorb the residual damping oil on the surface of the main spring.
- The main spring was then cut in half using a bandsaw, based on the recommendations in ISO:23539 standard [16]. The cutting speed was set to 20 mm/min to avoid large deformation and overheating for the elastomeric components during the cutting process.

The cross-section of the main spring, which is 1 mm offset to the central axis of the engine mount, was used to observe the internal strain distribution. The main reason for this choice is as follows: the stiffness of an engine mount is dominated by its main spring component. Since the load-carrying element in this spring is axisymmetric, any axisymmetric cross-sectional surface can be used to represent the strain distribution of the entire engine mount. The threaded hole in the tip of the main spring makes it convenient to connect the samples to the test machine mechanically to enable the hole to still be used after cutting. Therefore, a 1 mm offset was selected when preparing the test samples to maintain this connection method. An alternative connection method is to bond the half main spring sample on the compression plate using a HBM X60 ceramic adhesive. In this case, the offset-cutting arrangement would be to ensure sufficient bonding surface.

A layer of white paint was sprayed onto this cross-section followed by a layer of black speckles for DIC measurements. In this analysis, two digital Pixels Pike 170 cameras with a resolution of over five million pixels were set up at approximately 75 ^{o} to the given surface of engine mount, as shown in Figure 2.

Figure 2: Static compression test rig with digital image correlation

The choice of a two camera set-up is based on a preliminary study of out-of-plane displacement measurements recorded for a service-aged mount subjected to a static compression between 0 to 4 mm - see Figure 3. Out-of-plane displacements result from the bulging, under compression, of the free surface generated after the main spring was cut in half. Since the main spring has a significant out-of-plane deformation, a set-up with two cameras is needed for accurate calculation of in-plane strain values. In this study, the VIC-3D correlation software by Correlated Solutions Inc. was used to calculate the displacement vectors, and hence the strain distribution on the cross-sections. In order to evaluate the accuracy of the maximum principal strain, several images were captured without applying static compression. A correlation algorithm [17] was then used to identify the noise for maximum principal strain measurements. Based on these measurements, the strain accuracy was found to be approximately $163e^{-6}$.

Figure 3: Typical maximum out-of-plane displacements for a service-aged engine mount

3. Results

3.1. Stiffness of the entire engine mount

When engine mounts age in a real vehicle, both thermal and dynamic loading have a great influence on stiffness variations. Thermal ageing has been shown to be linked with ageing time and operating temperature [5]. Dynamic loading over a certain period of time on an engine mount may lead to permanent creep deformation. In a service-aged engine mount, this deformation can be represented by the initial gaps (see Table 1). The load-deflection relationship for the engine mounts under four different ageing conditions are illustrated in Figure 4.

Figure 4: Load-deflection data for the selected engine mounts

Close examination on the relationships between physical properties and linear stiffness of the engine mounts for different conditions are shown in Table 2. Due to the limited number of samples tested here there may be a correlation between working mileage and stiffness but more tests would be required to know for certain.

Table 2: Linear stiffness for the engine mounts at different working conditions

Sample	ageing condition	linear stiffness, N/mm
1	new	297
2	thermally-aged	369
3	service aged – 129,996 km	371
4	service aged – 70,600 km	432

3.2. Strain distributions of thermally-aged engine mounts

It has been widely accepted that thermal ageing of the elastomer influences the elastic modulus and, therefore, the stiffness of the engine mount [7]. However, limited research has been conducted on the influences of thermal effects on the geometric and micro-structural change inside the main spring of engine mounts. Comparison of strain distributions between the new and the thermally-aged engine mount are shown in Figure 5, where it can be seen that the magnitude and distributions of the Lagrange maximum principal strain remain similar between new and thermally-aged mounts, regardless of the amount of the applied static compression.

Figure 5: Maximum principal strain distributions in the main spring for both new and thermally-aged engine mounts when subjected to different amounts of static compressions

3.3. Stiffness variations of service-aged engine mount main springs

3.3.1. Static compression tests

As explained in Section 2.3, the main spring was cut into two pieces in order to carry out the DIC measurements. Static compression tests on the half main spring were also carried out for engine mounts with three different working conditions (Samples 1, 3 and 4). Results are shown in Figure 6.

Figure 6: Load-deflection data for the main springs with different service mileages

Compared to a new engine mount, the stiffness of service-aged mounts is significantly higher. Detailed tangent stiffness values at selected static compressions of the cut main springs are given in Table 3.

Table 3: Tangent stiffness of the cut main springs at selected static compressions

Static compression, mm		0.5	1	1.5	2	2.5	3
Stiffness, N/mm	Sample 1	94	106	100	100	100	95
	Sample 3	145	152	171	159	157	170
	Sample 4	129	125	150	150	150	175

Table 3 quantifies how significant the stiffening is with static compressions for service-aged samples.

3.3.2. Geometric variations

Significant differences of the initial gap can be observed for engine mounts under different ageing conditions - see Table 1. In order to investigate the cause of this difference, the DIC measurement was used to identify the original shape of the main springs under different ageing conditions. A small static compression of 0.08 mm was applied on the tip of the main spring to ensure the quality of this correlation.

Figure 7: Comparisons of the main spring geometries for the engine mounts in three different ageing conditions

Results are illustrated in Figure 7, where it can be seen that the main springs in service-aged mounts have experienced significant permanent creep deformation and, therefore, have much lower unladen heights. No significant correlations between the working mileage and deformation level can be found for the same type of engine mount due to the limited sample range. Additionally, the largest deformation of the service-aged samples always appears in the underside of the tip.

3.3.3. Strain distributions for service aged mounts

DIC measurements were conducted on service-aged engine mounts in order to identify the ageing mechanisms responsible for these stiffness variations.

Figure 8: Cross-sectional maximum principal strain distribution for main springs at different ageing conditions

It can be seen from Figure 8 that the area with high principal strain values shifts towards the tips of the main spring for the two aged mounts. For the engine mount with the highest mileage (sample 3), additional high principal strain regions appear in the topside of the rib.

4. Discussion

This section discusses the ageing mechanics for a service-aged engine mount first. Following this, the feasibility of a laboratory accelerated thermal ageing test to represent the real ageing behaviour of the engine mount is investigated.

4.1. Ageing mechanics of a real engine mount

Influences of thermal effects on an engine mount have been investigated widely [5,11,14]. Figure 5 also indicates that the DIC measurement has a limited capability to identify these changes. Therefore, this is not the focus of this paper. Instead, this paper considers the influences of geometric and micro-structural variations on the stiffness due to service ageing.

4.1.1. Developments of contact regions

Generally, new engine mounts exhibit a lower stiffness and more linear behaviour than the service-aged samples. One possible explanation for the static compression-dependent stiffening for service-aged samples observed during testing is geometric nonlinearity, specifically via the development of contact regions during service-ageing - see Figure 9. Stiffening is expected to increase as a result because more regions inside engine mounts carry loads transferred from the engine.

Figure 9: Development of contact regions for service-aged engine mounts

A comparison of the maximum principal strain distributions between a new mount with large deformation and the corresponding service-aged mount is shown in Figure 10. Note that the final height of both cut main springs is approximately 72 mm.

Figure 10: Maximum principal strain distribution at the same height of 72 mm: (a) Sample 1 (New) under 11 mm of static compression deflection and (b) Sample 3 (service-aged with mileage of 129,996 km) under 1 mm of static compression deflection

The high strain region for the new aged mount is located in the top side of the ribs in the main spring even when the final height is similar to the service-aged ones. Meanwhile, this region shifts towards the tips for a service-aged mount. This result reiterates the development of unexpected contacts due to a significant visible change of the shape of the mounts after a long time in service.

4.1.2. Creep deformation

In service-aged samples, the main springs experience significant permanent creep deformation because dynamic loading contributes to the ageing of the engine mount in practical working conditions. Although this creep phenomenon would not affect the elastic modulus of the material significantly [18], it can change the shape of the load-carrying region and, therefore, the stiffness of the engine mount.

The chemical creep deformed shape of the cross-section differs from that obtained purely from high static compression. This is illustrated in Figure 11. where the geometry of an aged engine mount after 129,996 km is compared to the shape of the new engine mount after application of a large static compression to ensure the two engine mounts have the same final height.

Figure 11: Comparisons of the main spring geometries: static v.s. creep deformation

Note that the deformed edge of a new engine mount is not identified in the vertical position higher than 73 mm due to the quality of speckle painting. It can be seen from Figure 11 that the creep deformation was developed in the underside of the tip. Meanwhile, the main load-carrying region for a pure static compression is in the top side of the ribs. As a result, the structural integrity for a real service-aged mount differs from the new one with same unladen height.

4.1.3. Micro-structural change

For the engine mount with the highest mileage, additional high principal strain regions appear - see Figure 10. This feature appears to link with micro-structural change and could potentially explain the drop in stiffness recorded for this mount in Figure 6. The underlying mechanics may be as follows. The dynamic loading will couple with the resonance of the load-carrying region. As a result, high dynamic strain will be achieved in this region. With the increase in mileage, the probability of damage appearing in the main spring increases. For a very high mileage, this could eventually lead to a possible stiffness decrease. In summary, creep deformation as well as thermal effects makes the material become inhomogeneous in the main spring of a service aged mount.

4.2. Feasibility study of laboratory ageing tests

The previous section demonstrates the importance of the geometric and micro-structural variations on the stiffness of a service-aged mount. However, this behaviour was always studied using a laboratory thermal ageing test. The underlying assumption is that temperature-dependent stiffness variations for the elastomers inside the mount occupies a central position for service ageing. From the observations in this study, it can be interpreted that pure thermal effects would change the elastic modulus of the elastomers inside the engine mount uniformly. Comparisons of the maximum principal strain pattern between Figure 5 and 8 indicate accelerated ageing tests with pure thermal effects do not simulate correctly real ageing conditions experienced by service-aged engine mounts.

4.3. *Measurement limitations*

Due to practical difficulty in supplying a large number of engine mounts, especially from used vehicles, results reported in this work are restricted to four samples representing four different ageing conditions. A larger number of tests would be needed to confirm the trend found in this study, especially for engine mounts with high mileage. Uncertainties in measurements are also difficult to quantify through repeated tests as it is almost impossible to retrieved engine mounts with exactly the same ageing conditions. All the aged mounts were indeed disassembled from real vehicles with ageing conditions likely to differ in terms of time in service and environment (e.g. temperature and humidity). However, the DIC approach developed in this study has demonstrated that strain field measurements carried out for a limited number of retrieved engine mounts can provide new insight into their ageing mechanisms.

5. Conclusions

A new experimental procedure has been successfully developed to study ageing of engine mounts under real and practical conditions by analysing the evolution of geometry of the elastomeric main spring and its internal strain distribution. The DIC observations have provided a new insight into identifying the ageing mechanics of a service-aged engine mount.

Specifically, the laboratory tests of accelerated thermal ageing samples indicate that the material ageing for the main spring is uniform and homogeneous and, therefore, can be represented using a nonlinear elastic modulus relationship. The DIC observations demonstrate that the strain distribution varies with ageing mileage. This new result suggests that the stiffening is caused non-uniformly. A secondary factor that was observed and thought to contribute, at least in part, was the development of additional contact areas.

Meanwhile, the origin of the softening of the engine mount for a very high mileage is still not clear. However, the experimental observations in the paper suggest that it may be caused by a combined effect of two material ageing phenomena: creep deformation of the load-carrying region and micro-structural change. When the service mileage of an engine mount is high, the internal strain distribution indicates that the number of high-strain regions increase. This observation indicates that micro-structural change is highly likely to have occurred, in which case it would contribute to a reduction in the overall stiffness of the mount.

To conclude, the results show that chemical creep deformation and the inhomogeneous elasticity of the main spring are of great importance in designing the overall life cycle for an engine mount. The classic thermal accelerated ageing test method has been shown to fail in predicting these features. As a result, it is suggested that, a high-temperature fatigue testing method is needed to simulate the service ageing. This is an area for future work.

Acknowledgements

The authors would like to acknowledge the support by Jaguar Land Rover and the EPSRC via Grant EP/L025752/1 as part of the jointly funded Programme for Simulation Innovation (PSi).

Data availability

The raw and processed data required to reproduce these findings cannot be shared at this time due to technical limitations related to file size for DIC data sets. Data is available upon request.

References

[1] H. Yarmohamadi, V. Berbyuk, Computational model of conventional engine mounts for commercial vehicles: validation and application, Vehicle System Dynamics 49 (2011) 761–787.

[2] L. Ooi, Z. Ripin, Optimization of an engine mounting system with consideration of frequency-dependent stiffness and loss factor, Journal of Vibration and Control 22 (2016) 2406–2419.
[3] L. E. Ooi, Z. M. Ripin, Dynamic stiffness and loss factor measurement of engine rubber mount by impact test, Materials & Design 32 (2011) 1880 – 1887.
[4] P. Soltani, C. Pinna, D. Wagg, R. Whear, Ageing simulation of a hydraulic engine mount: A data-informed finite element approach. Proceedings of the Institution of Mechanical Engineers, Part D: Journal of Automobile Engineering, (2018).
[5] F. Ngolemasango, M. Bennett, J. Clarke, Degradation and life prediction of a natural rubber engine mount compound, Journal of Applied Polymer Science 110 (2008) 348–355.
[6] A. Ahagon, M. Kida, H. Kaidou, Aging of tire parts during service. i. types of aging in heavy-duty tires, Rubber Chemistry and Technology 63 (1990) 683–697.
[7] R. Conley, Thermal Stability of Polymers: In 2 Vols, volume 1, Marcel Dekker, 1970.
[8] J. Willett, K. O'Connor, R. Wool, The role of chain scission in fracture of amorphous polymers, Journal of Polymer Science Part B: Polymer Physics 24 (1986) 2583–2589.
[9] K. T. Gillen, M. Celina, R. Bernstein, Validation of improved methods for predicting long-term elastomeric seal lifetimes from compression stress relaxation and oxygen consumption techniques, Polymer Degradation and Stability 82 (2003) 25 – 35.
[10] A. Chai, A. Andriyana, E. Verron, M. Johan, Mechanical characteristics of swollen elastomers under cyclic loading, Materials & Design 44 (2013) 566 – 572.
[11] H. Chou, J. Huang, Effects of cyclic compression and thermal aging on dynamic properties of neoprene rubber bearings, Journal of Applied Polymer Science 107 (2008) 1635–1641.
[12] T. Naruse, T. Hattori, Y. Yamaguchi, T. Kanai, T.Sekiya, Thermal degradation of chlorosulfonated polyethylene rubber and ethylene propylene diene terpolymer, Materials & Design 42 (2012) 147 – 155.
[13] S. Kashi, R. Varley, M. Souza, S. Al-Assafi, A. Pietro, C. Lavigne, B. Fox, Mechanical, thermal, and morphological behavior of silicone rubber during accelerated aging, Polymer-Plastics Technology and Engineering 0 (2018) 1–10.
[14] W. Mars, A. Fatemi, Factors that affect the fatigue life of rubber: A literature survey, Rubber Chemistry and Technology 77 (2004) 391–412.
[15] W. Mars, A. Fatemi, Fatigue crack nucleation and growth in filled natural rubber, Fatigue & Fracture of Engineering Materials & Structures 26 (2003) 779–789.
[16] ISO 23529:2016, Rubber – General procedures for preparing and conditioning test sieces for physical test methods, Standard, International Organization for standardization, Geneva, CH, 2016.
[17] H. Schreier, J. Orteu, M. Sutton, Image correlation for shape, motion and deformation measurements, Springer US, 2009.
[18] L. W. McKeen, The effect of long term thermal exposure on plastics and elastomers, William Andrew, 2013.

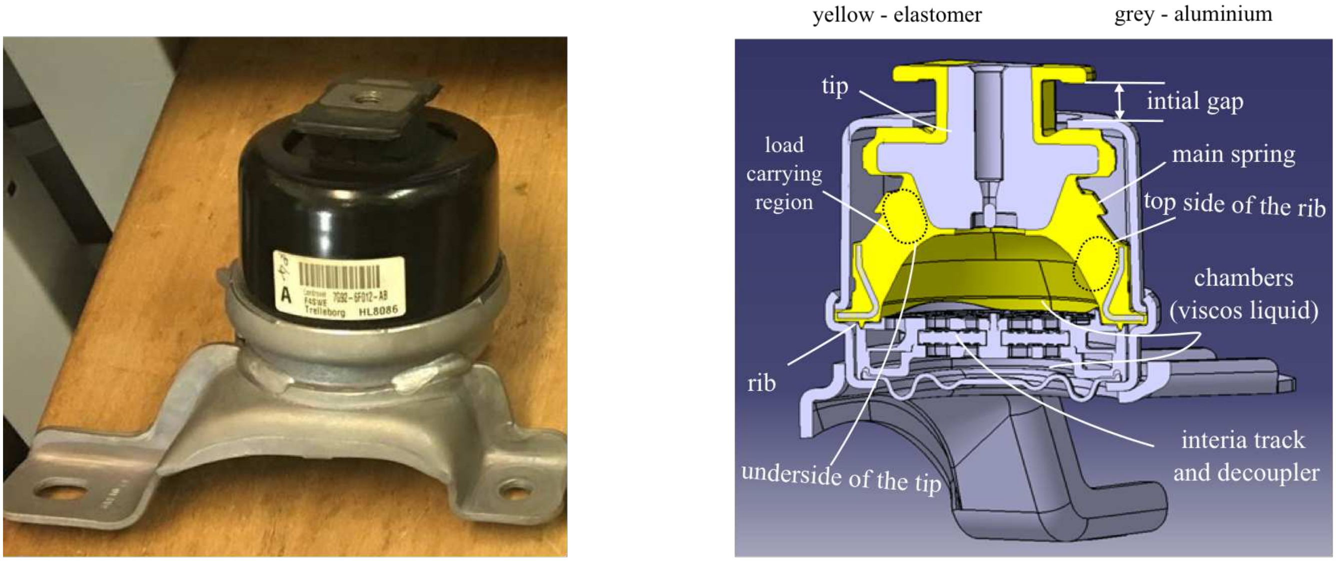

(a) hydraulic engine mount (b) cross-sectional view

Figure 1: Hydraulic engine mount and its components.

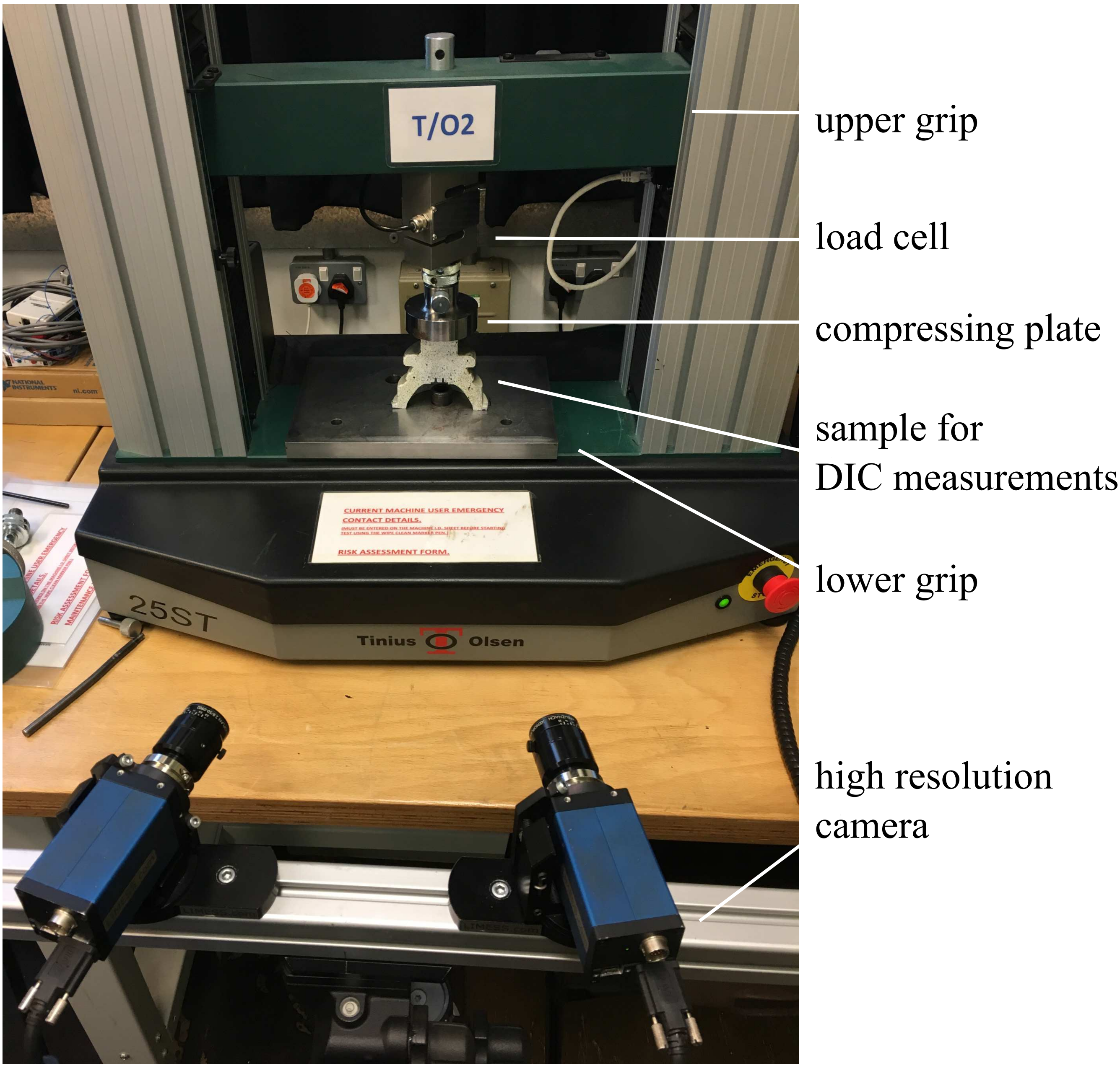

Figure 2: Static compression test rig with digital image correlation

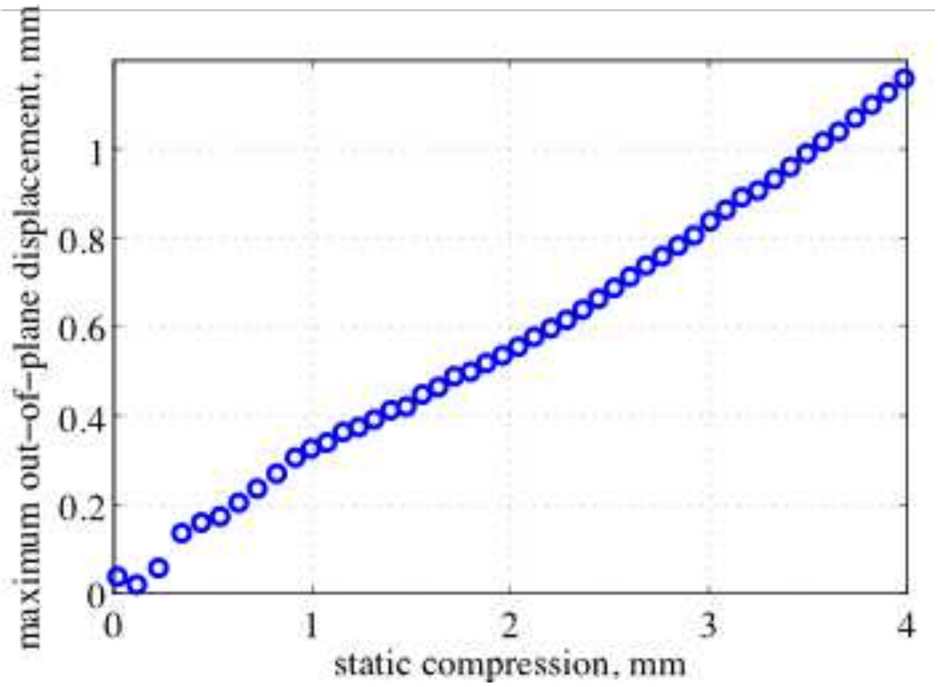

Figure 3: Typical maximum out-of-plane displacements for a service-aged engine mount

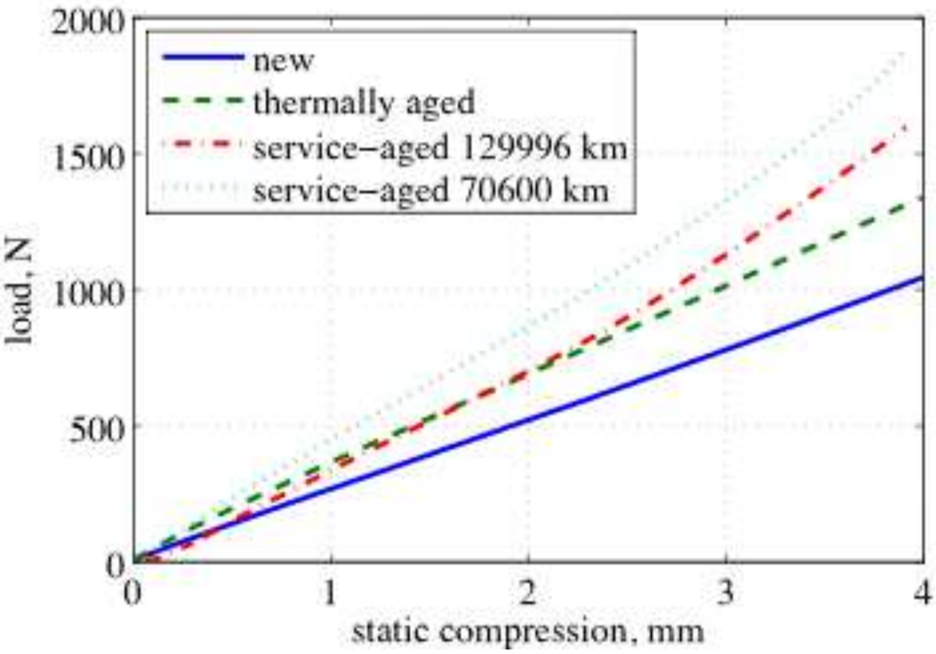

Figure 4: Load-deflection data for the selected engine mounts

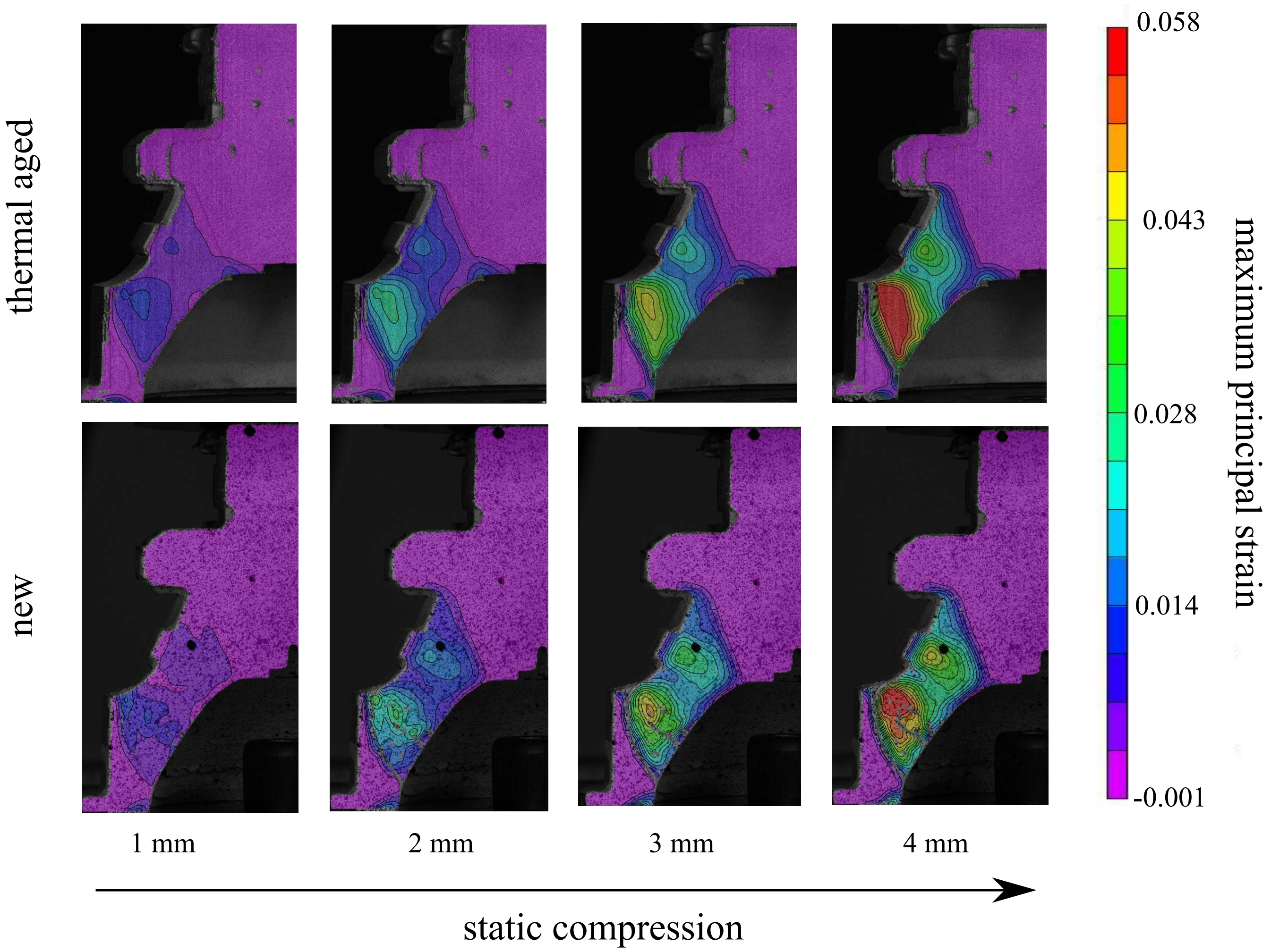

Figure 5: Maximum principal strain distributions in the main spring for both new and thermally-aged engine mounts when subjected to different amounts of static compressions

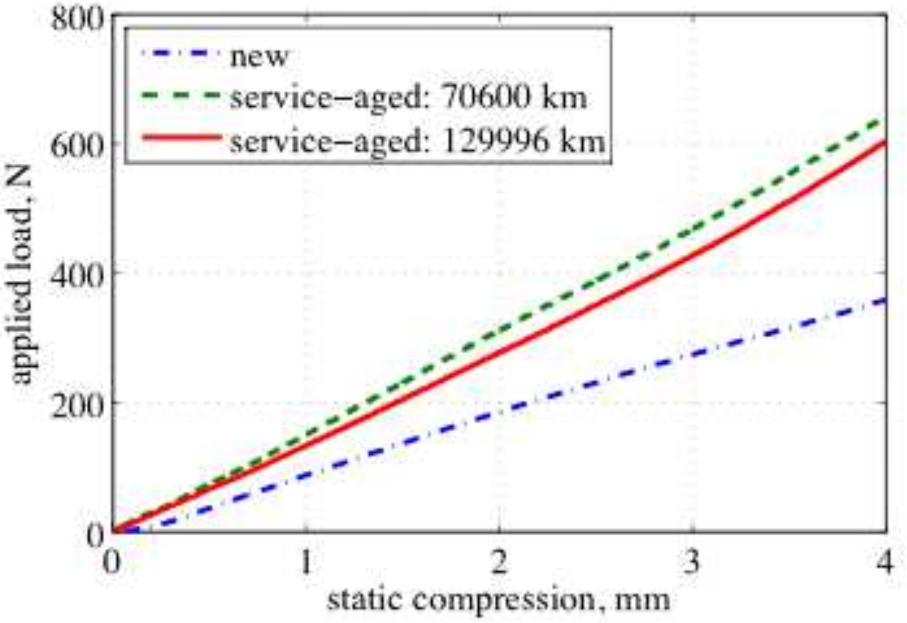

Figure 6: Load-deflection data for the main springs with different service mileages

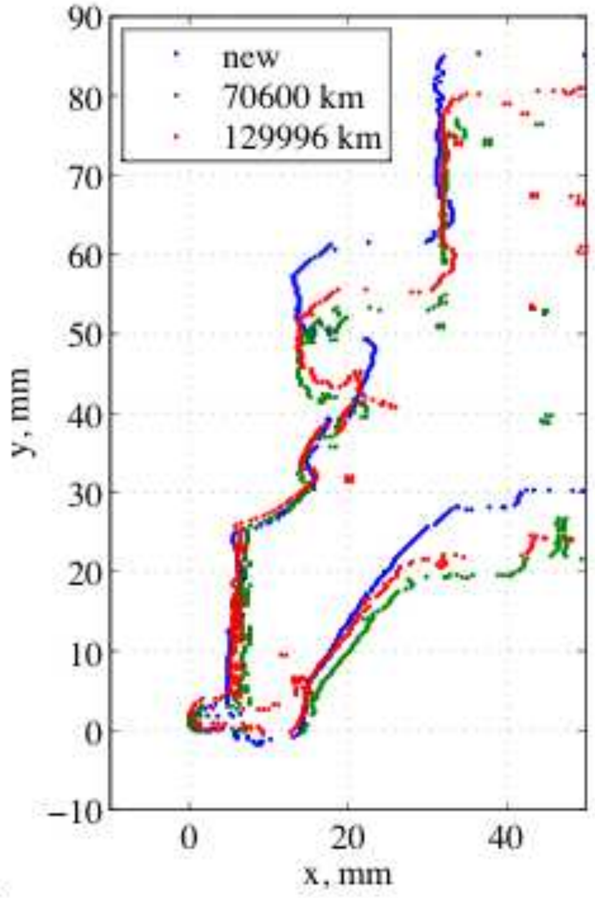

Figure 7: Comparisons of the main spring geometries for the engine mounts in three different ageing conditions

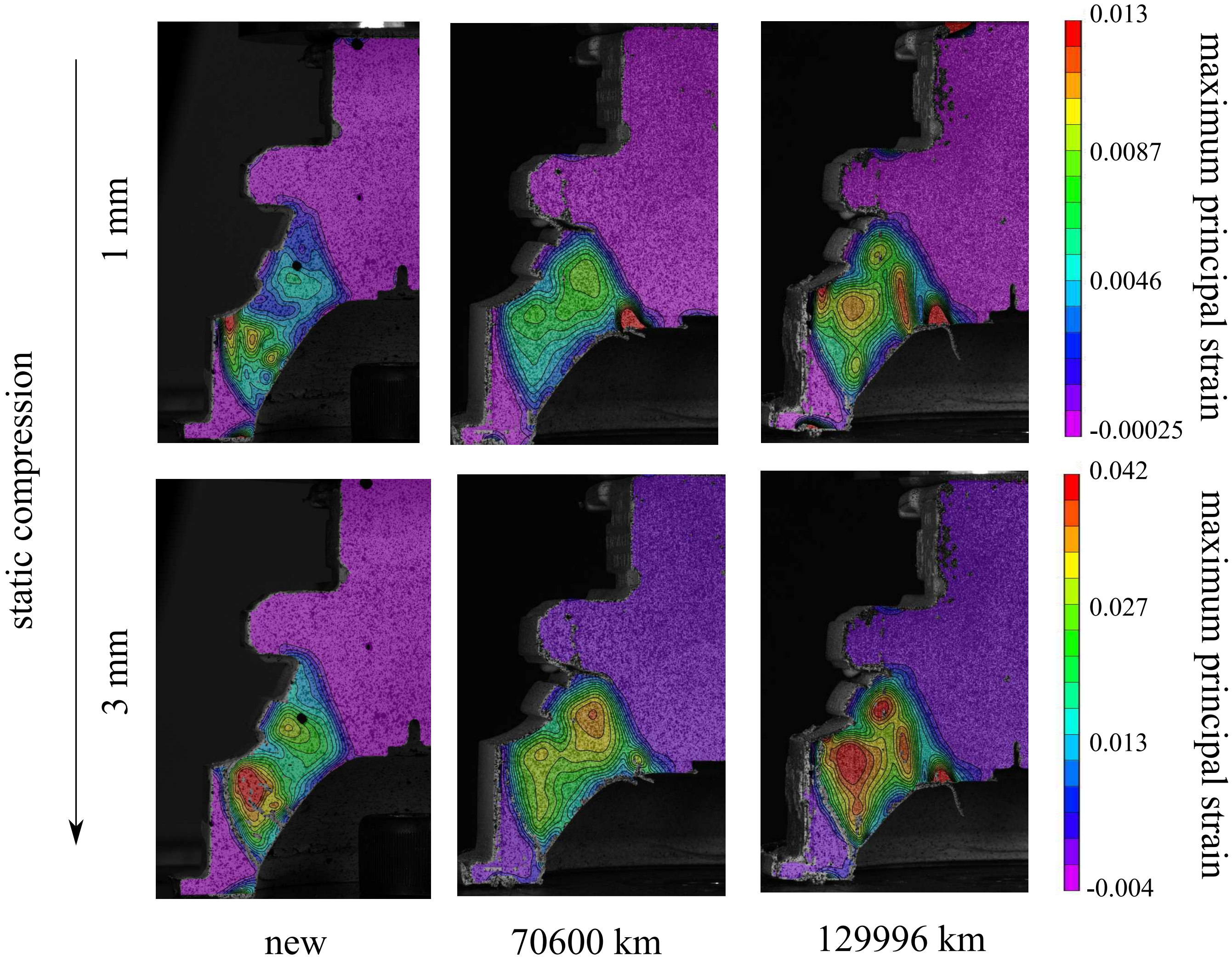

Figure 8: Cross-sectional maximum principal strain distribution for main springs at different ageing conditions

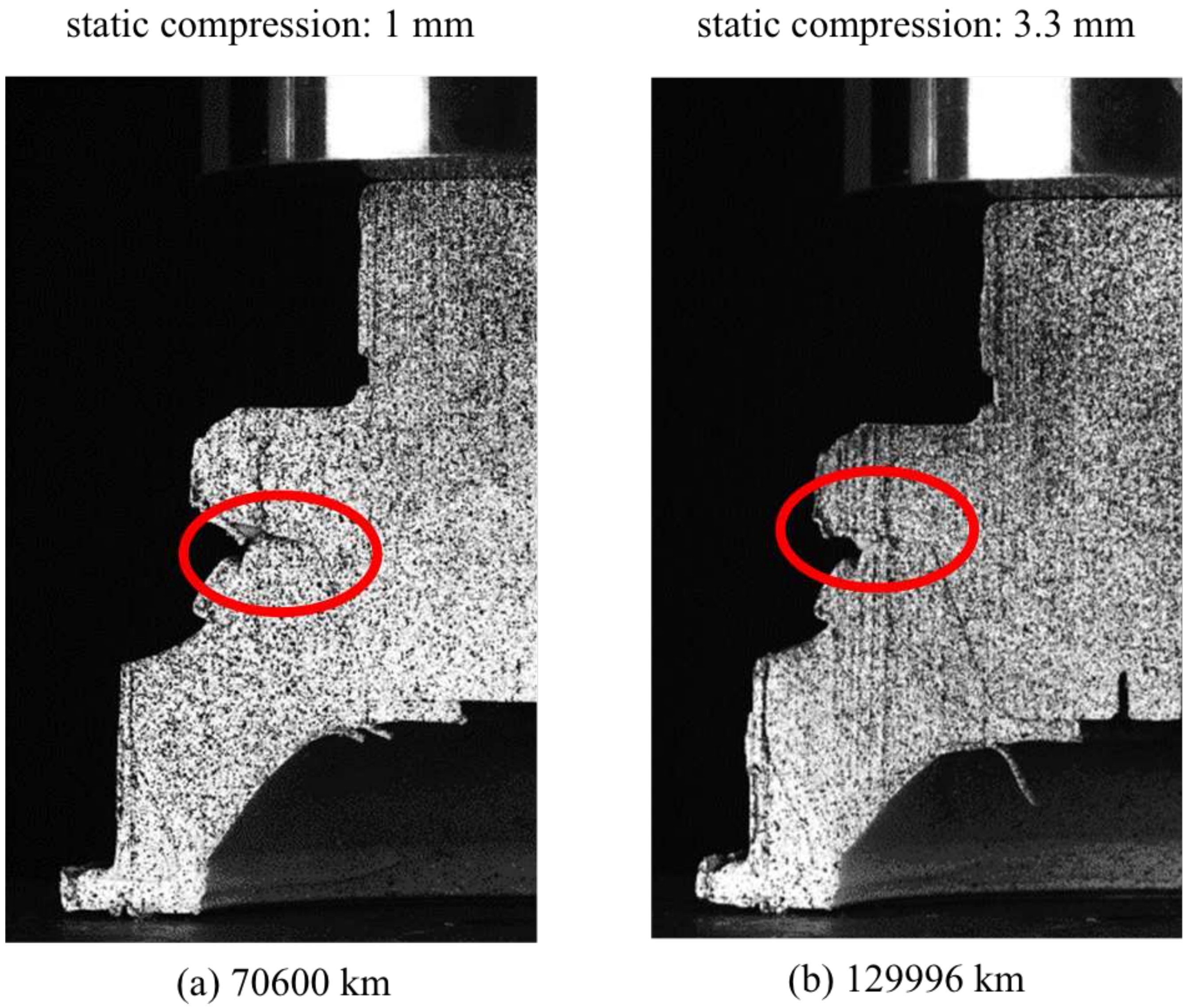

Figure 9: Development of contact regions for service-aged engine mounts

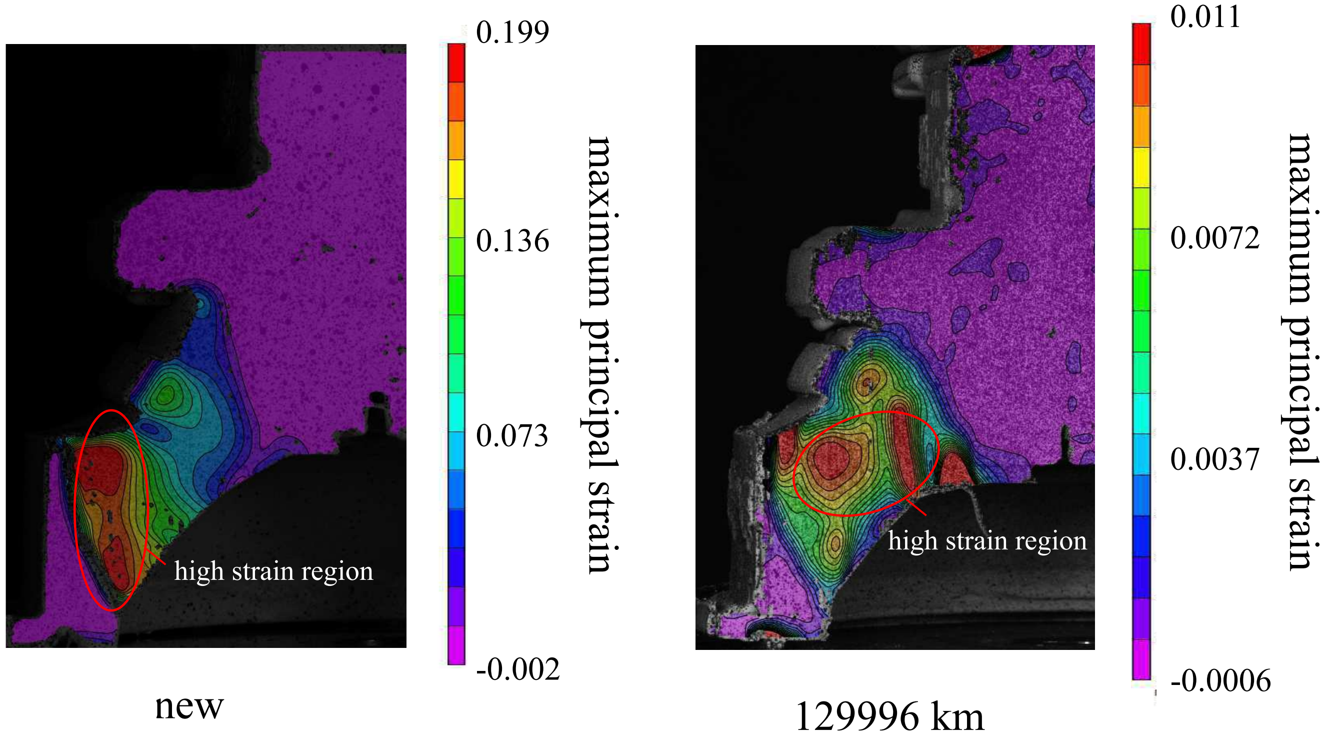

Figure 10: Maximum principal strain distribution at the same height of 72 mm: (a) Sample 1 (New) under 11 mm of static compression deflection and (b) Sample 3 (service-aged with mileage of 129,996 km) under 1 mm of static compression deflection

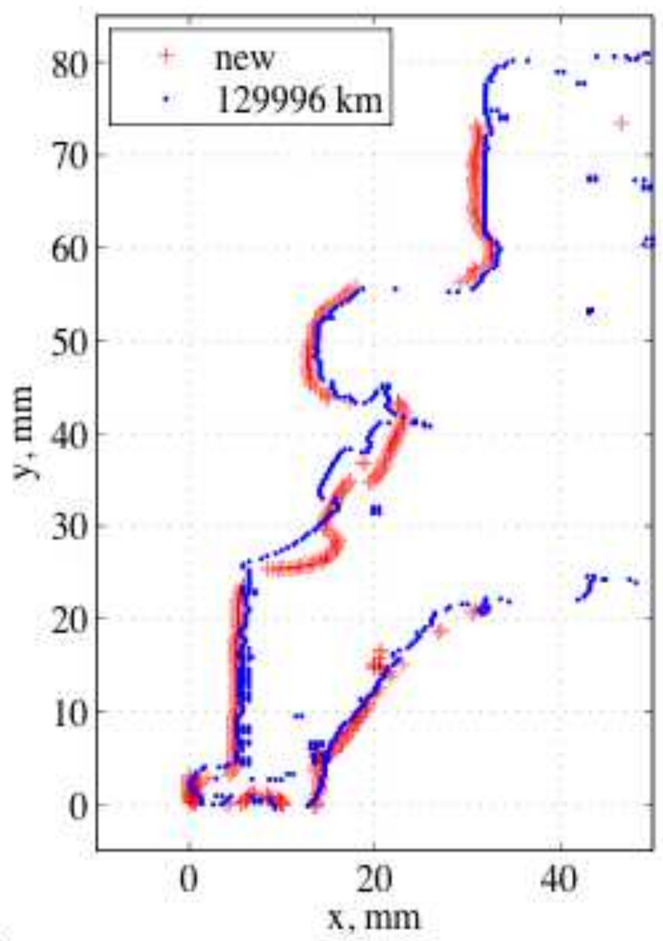

Figure 11: Comparisons of the main spring geometries: static v.s. creep deformation